Proceedings Paper:
Chen, L., Chen, X., Wang, J. orcid.org/0000-0003-4870-3744 et al. (1 more author) (2017) Computationally efficient, electro-thermally coupled model for permanent magnet machines in electric vehicle traction applications. In: UNSPECIFIED SAE Thermal Management Systems Symposium, TMSS 2017, 10-12 Oct 2017, Plymouth, MI, USA. .

COMPUTATIONALLY EFFICIENT, ELECTRO-THERMALLY COUPLED MODEL FOR PERMANENT MAGNET MACHINES IN ELECTRIC VEHICLE TRACTION APPLICATIONS

Liang Chen, Xiao Chen, Jiabin Wang and Antonio Griffo,
University of Sheffield, UK

Outline

- Research Motivation
- Methodology (Equivalent d-axis current representing temperature effect)
- Electro-thermally Coupled Model
- FE Validation
- Simulation Results
- Experimental Validation

Research Motivation

- ❑ **Electrical machine temperatures are subject to its copper loss, core loss, etc.**
- ❑ **Machine copper loss and core loss are largely affected by machine temperatures**

a) Winding resistance increases by 39% for every 100^{o}C temperature rise;

b) Magnet remanence reduces by 12% for every 100^{o}C temperature rise (for NdFeB);

c) High nonlinearity in the machine flux linkage map due to core saturation

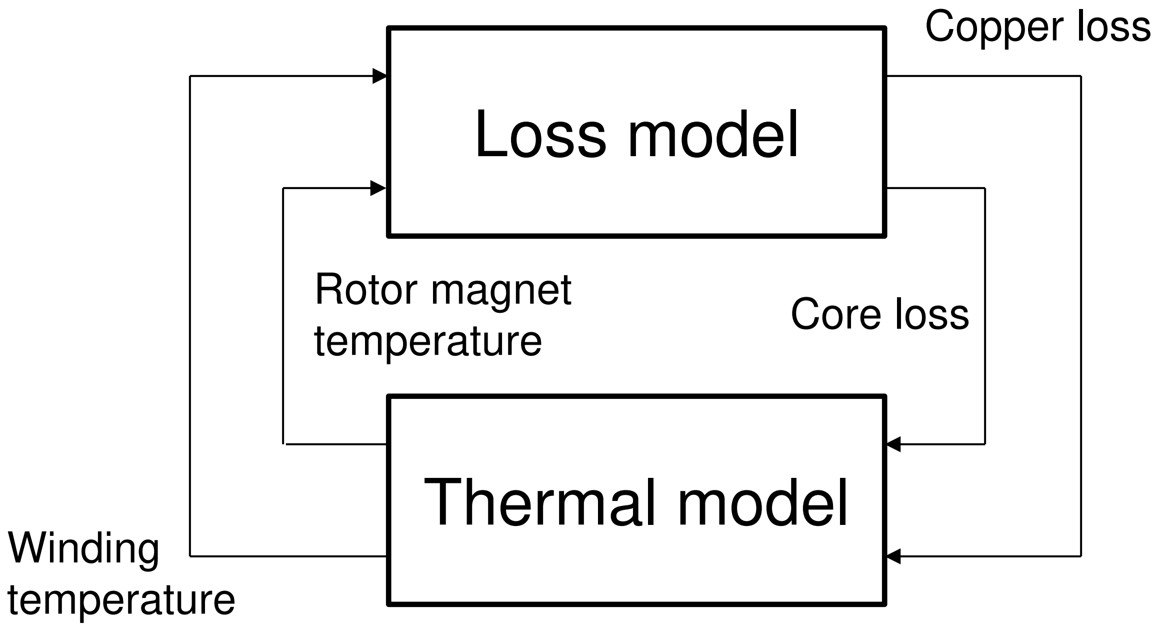

Research Motivation

- **Electrical machine temperatures are subject to its copper loss, core loss, etc.**
- **Machine copper loss and core loss are largely affected by machine temperatures**

a) Winding resistance increases by 39% for every 100°C temperature rise;

b) Magnet remanence reduces by 12% for every 100°C temperature rise (for NdFeB);

c) High nonlinearity in the machine flux linkage map due to core saturation

Essential to accurately model the electro-thermally coupling effect in the electrical machine, in order to accurately simulate the waste heat recovery in the vehicle powertrain system.

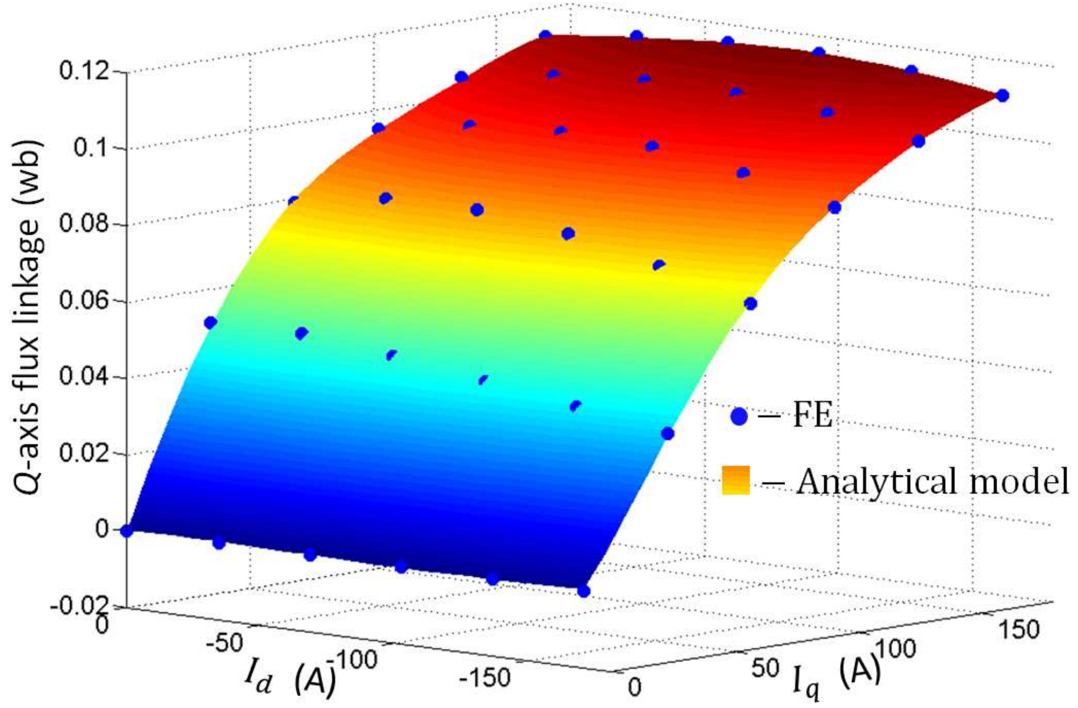

10kW 18-slot 8-pole IPM machine

Temperature Effects on Flux Linkages

$$B_{r2}(T_2) = B_r(T_1) \times [1 + \alpha \times (T_2 - T_1)]$$

where α is temperature coefficient, B_{r2} and B_{r1} represent the remanence at temperature of T_2 and T_1, respectively.

d-axis flux linkage increment over *d*-, *q*-axis current ranges when temperature decreases from 100°C to 20°C (normalized to the flux-linkage due to permanent magnets at 120°C)

The increment can be up to 18%;
The increment is non-uniform in the range of *d*- and *q*-axis currents

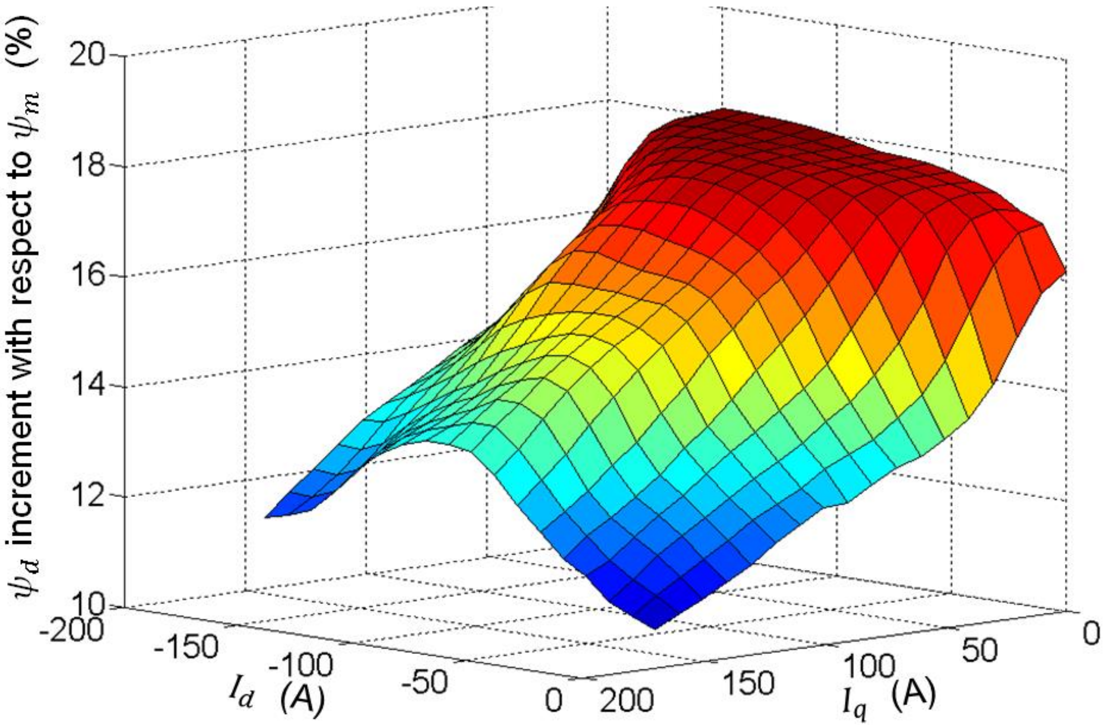

10kW 18-slot 8-pole IPM machine

Temperature Effects on Flux Linkages

$$B_{r2}(T_2) = B_r(T_1) \times [1 + \alpha \times (T_2 - T_1)]$$

where α is temperature coefficient, B_{r2} and B_{r1} represent the remanence at temperature of T_2 and T_1, respectively.

q-axis flux linkage increment over *d*-, *q*-axis current ranges when temperature decreases from 100°C to 20°C (normalized to the flux-linkage due to permanent magnets at 120°C)

Neglecting the temperature effect on the *q*-axis flux linkage does not incur large error

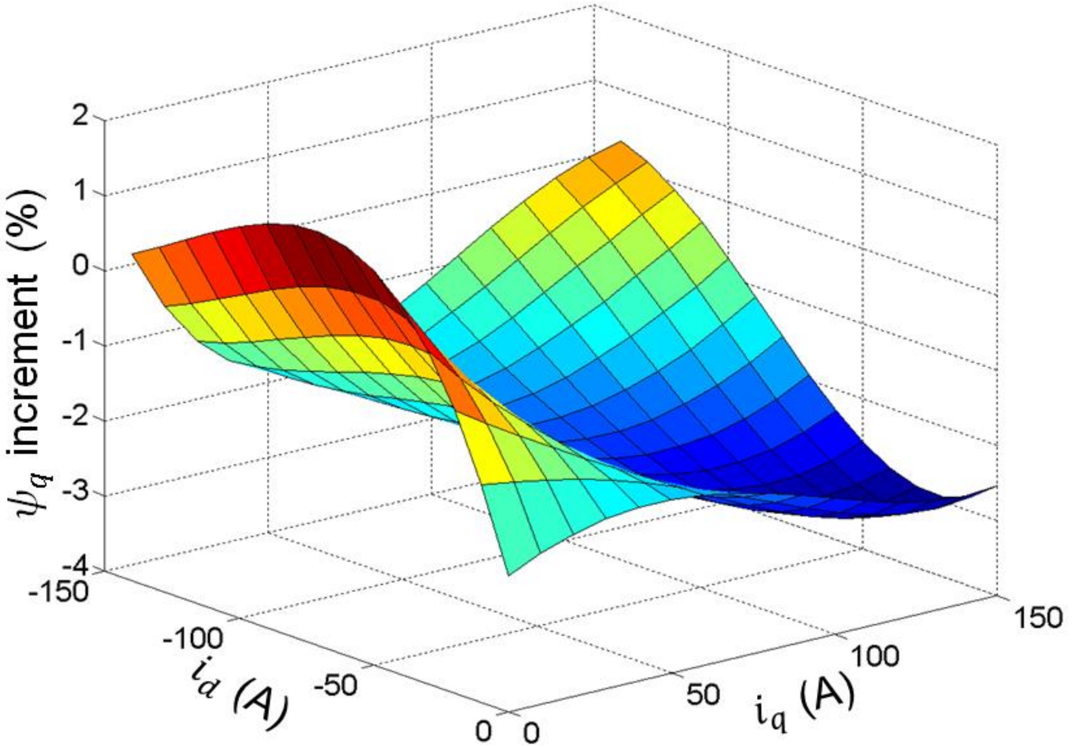

10kW 18-slot 8-pole IPM machine

Temperature Effects on Flux Linkages

$$B_{r2}(T_2) = B_r(T_1) \times [1 + \alpha \times (T_2 - T_1)]$$

where α is temperature coefficient, B_{r2} and B_{r1} represent the remanence at temperature of T_2 and T_1, respectively.

FE predicted open-circuit *d*-axis flux linkage ψ_d variation with magnet temperature.

Due to saturation effect, ψ_d varies not strictly linear with temperature

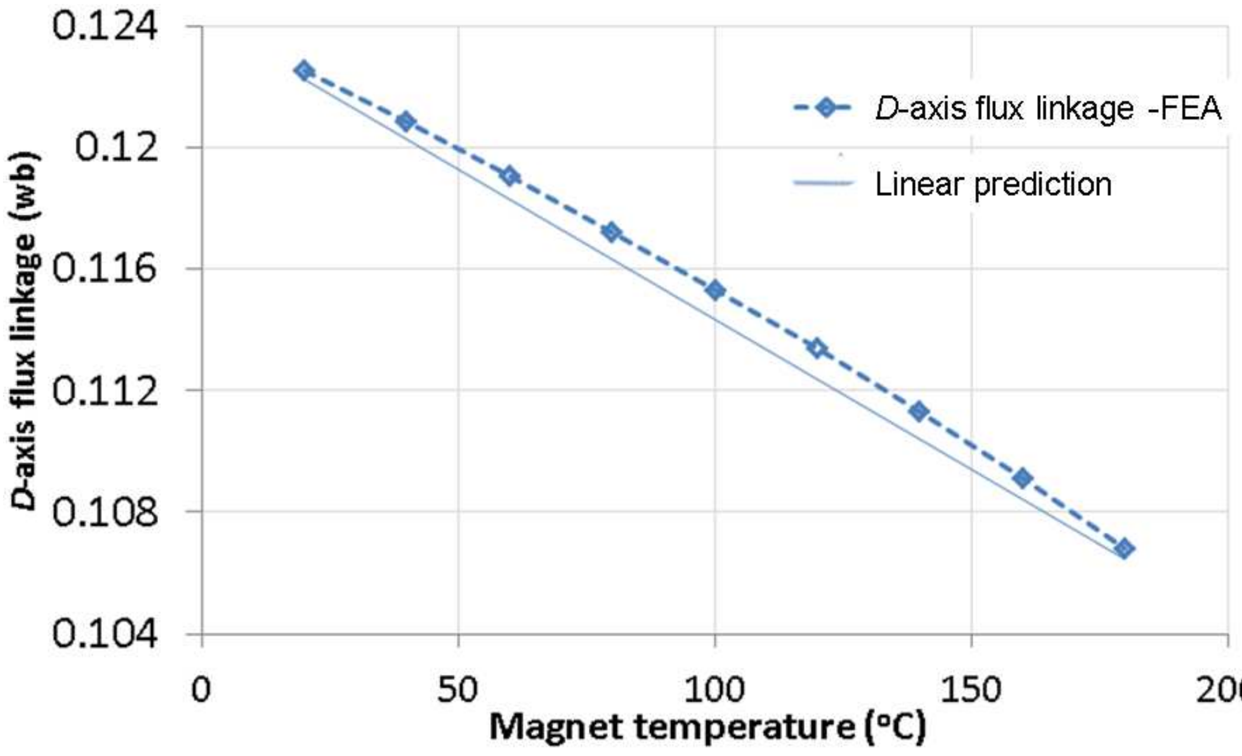

Equivalent d-axis Current Representing Temperature Effects

Magnetic flux path

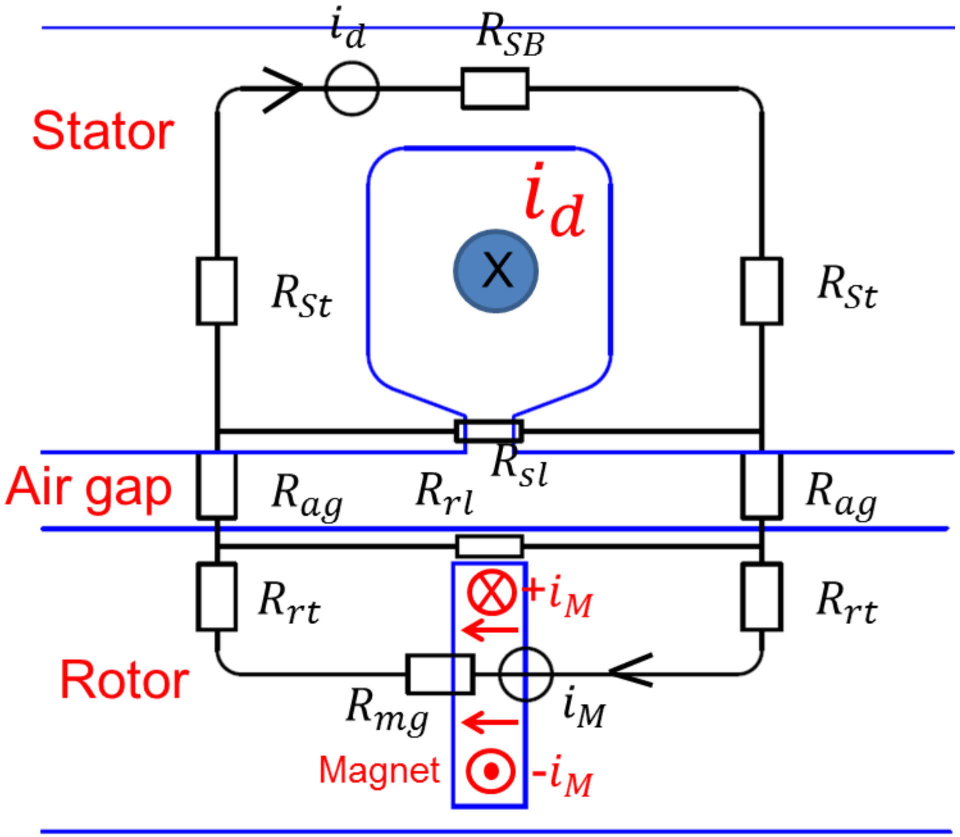

Equivalent magnetic circuit

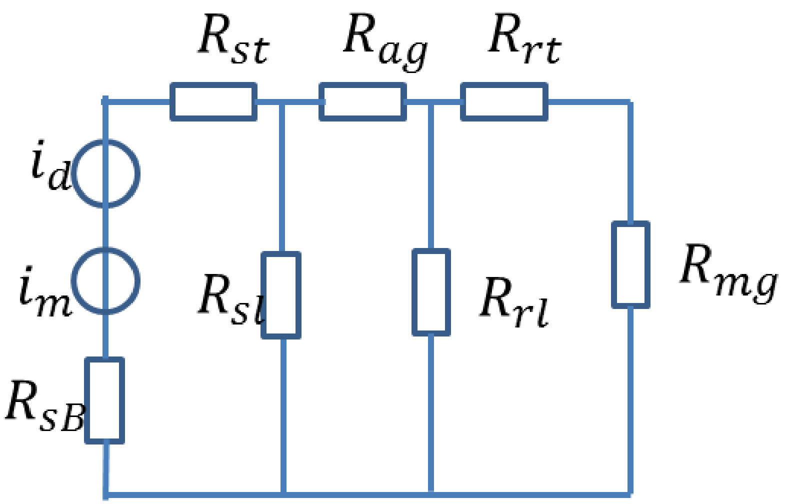

Therefore the total equivalent excitation current in the d-axis seen by the stator windings is $i_d + i_m$

i_m changes proportionally to the temperature variation

Equivalent *d*-axis Current Representing Temperature Effects

Therefore, when temperature changes,

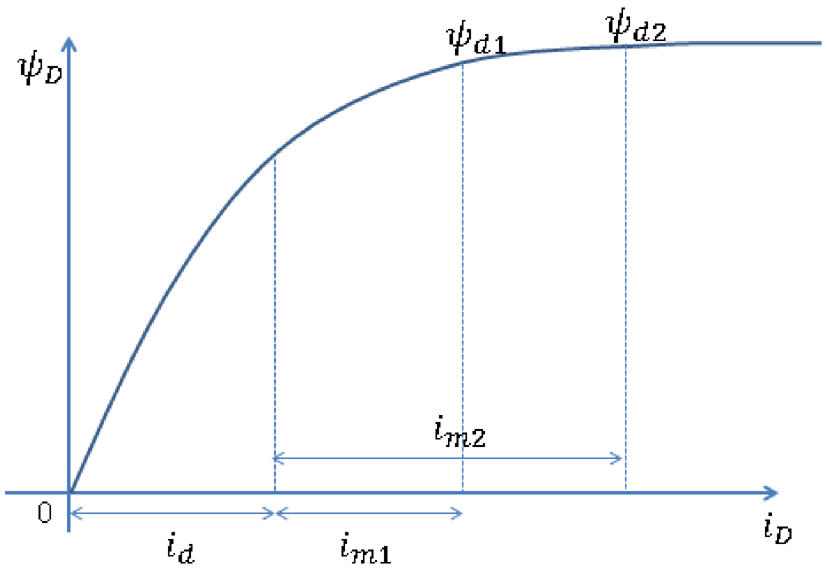

$$\psi_d(i_d, i_q, T_1) = \psi_D(i_d + i_{m1}, i_q)$$

$$\psi_d(i_d, i_q, T_2) = \psi_D(i_d + i_{m2}, i_q)$$

$$\begin{aligned}\psi_d(i_d, i_q, T_2) &= \psi_D(i_d + i_{m1} + i_{m2} - i_{m1}, i_q) \\ &= \psi_d(i_d + (i_{m2} - i_{m1}), i_q, T_1) \\ &= \psi_d(i_d + i_{mc}, i_q, T_1)\end{aligned}$$

where $i_{mc} = i_{m2} - i_{m1}$

Therefore the flux linkages at a new temperature T_2 can be predicted using the model at the reference temperature T_1 with its d-axis current displaced by a constant i_{mc}, which is equal to the magnet equivalent current difference between the two temperatures.

Equivalent *d*-axis Current Representing Temperature Effects

Considering the flux linkage variation due to different rotor position:

$$\psi_d(i_d, i_q, \theta, T_2) = \psi_d(i_d + i_{mc}, i_q, \theta, T_1)$$

$$\psi_q(i_d, i_q, \theta, T_2) = \psi_q(i_d + i_{mc}, i_q, \theta, T_1)$$

Neglecting the saturation effect in the rotor bridge region:

$$i_{mc} = i_{m2} - i_{m1} = i_{m1} \times \alpha \times (T_2 - T_1)$$

i_{m1} can be calculated using the short-circuit condition:

$$\psi_D(i_{d-sc1} + i_{m1}, 0) = \psi_d(i_{d-sc1}, 0, T_1) = 0$$

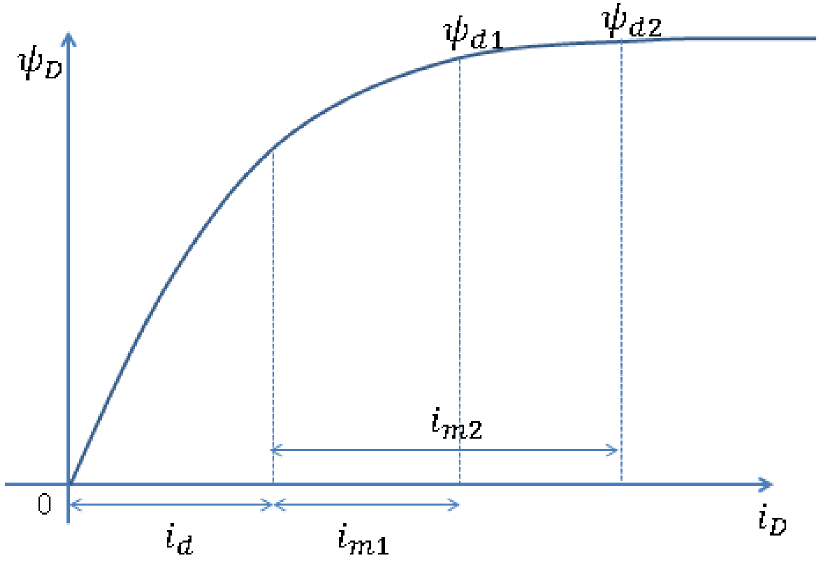

Once i_{m1} has been determined from the FE simulation of the short-circuit condition at the reference temperature T_1, the i_{mc} at any given temperature T_2 can be obtained.

Then, use the modified *d*-axis current $i_d + i_{mc}$ to calculate the flux linkages and torque at any temperature.

Inverse Flux Linkage Model with Temperature Effects

Conventional flux linkage model:

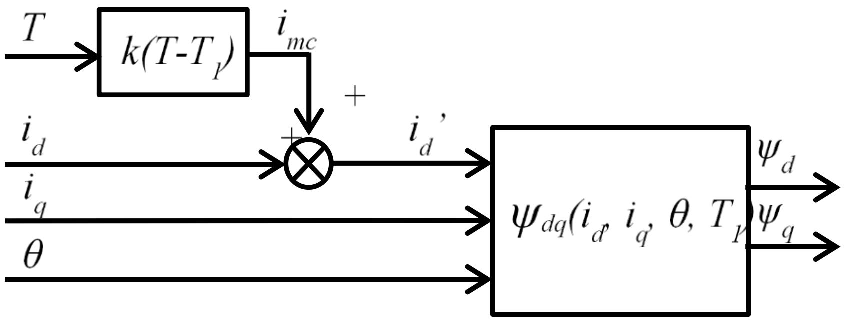

Inverse flux linkage model:

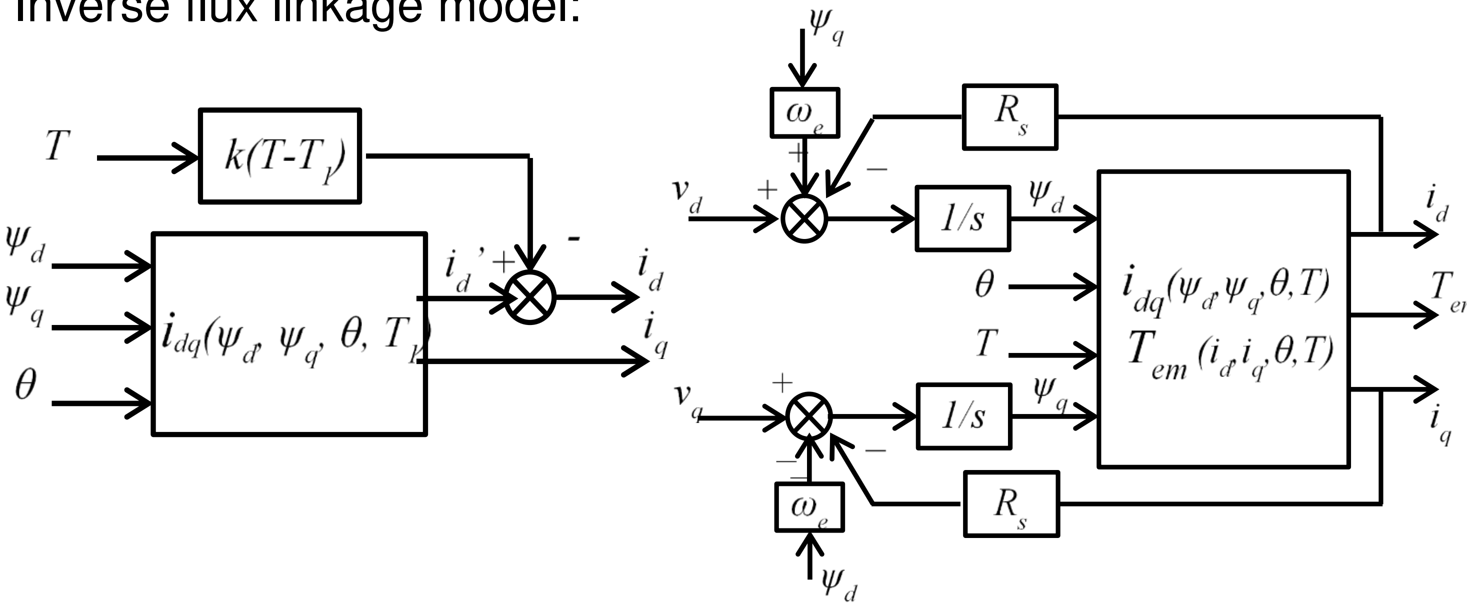

$$i_d(\psi_d, \psi_q, \theta, T) = i_{d1}(\psi_d, \psi_q, \theta, T_1) - k(T - T_1)$$

$$i_q(\psi_d, \psi_q, \theta, T) = i_{q1}(\psi_d, \psi_q, \theta, T_1)$$

FE Validation

d-axis flux linkage error

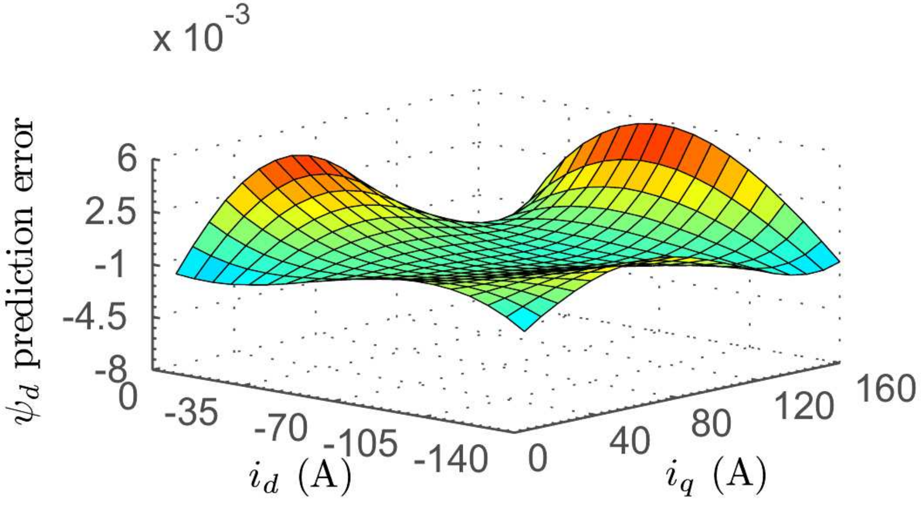

q-axis flux linkage error

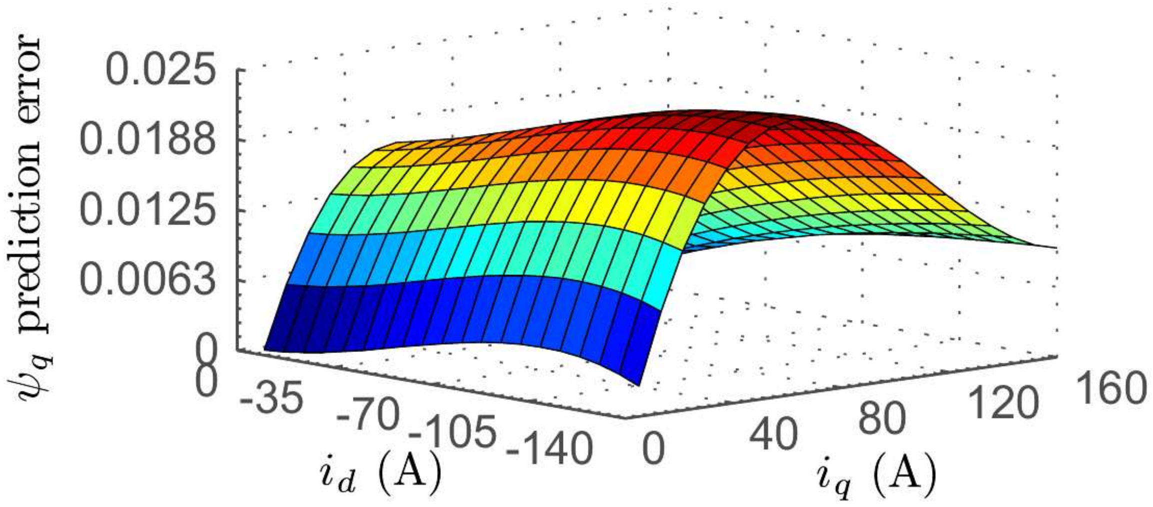

RMS error over i_d and i_q ranges:

Variables	% change (from 100 °C to 20 °C)	Relative error of proposed model
ψ_d	10.82%	1.41%
ψ_q	1.45%	1.51%
ψ_m	8.98%	1.28%
T_q	4.66%	0.98%

Time Domain Simulation

Rated torque and base speed (35Nm and 1350r/min)

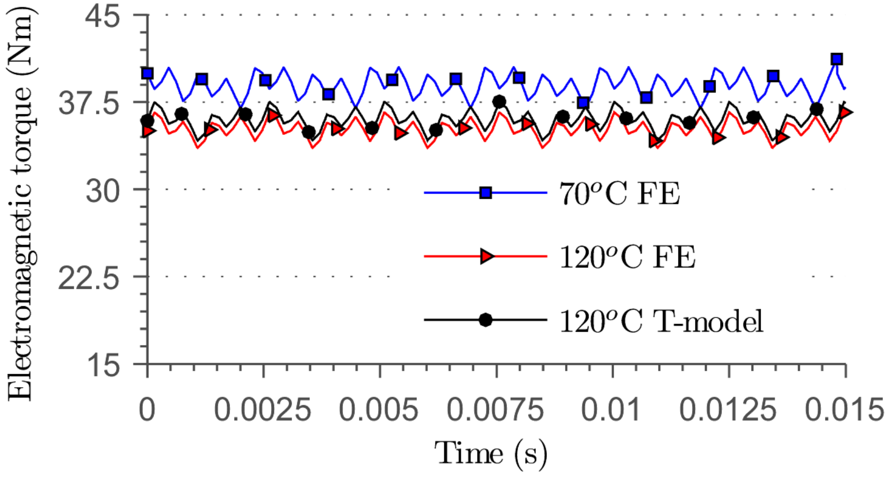

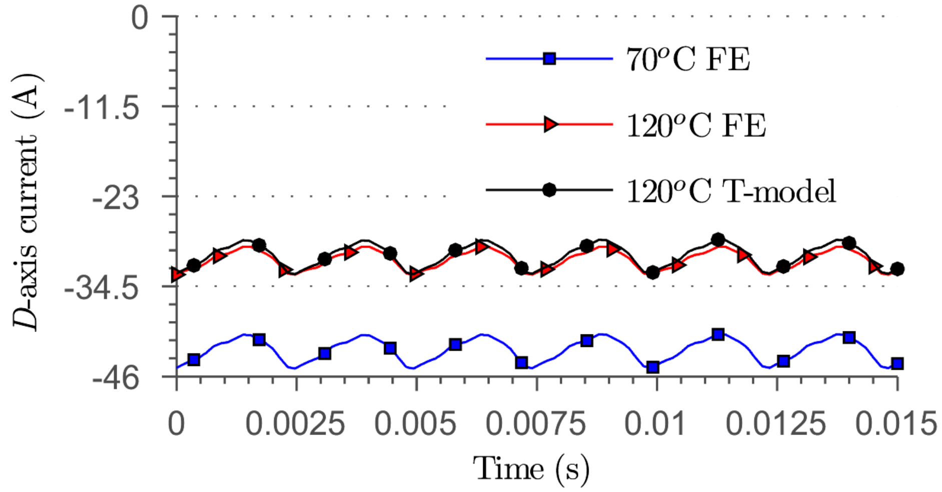

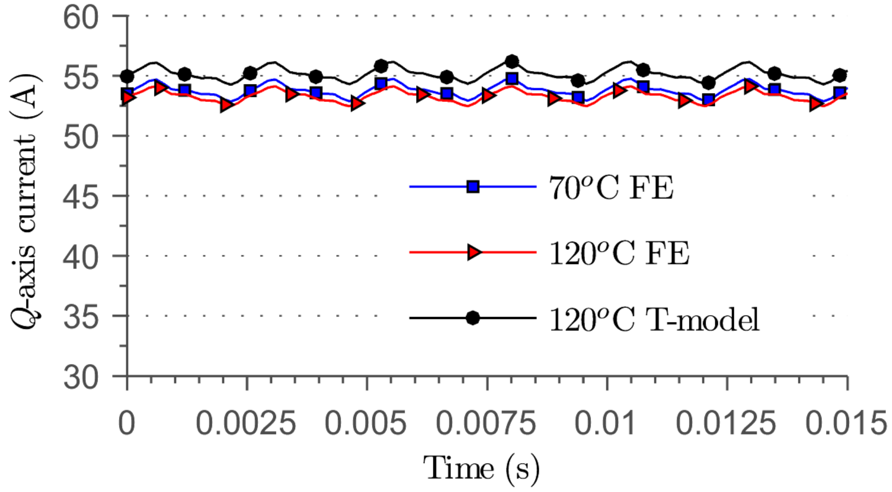

Good agreement achieved

Time Domain Simulation

Field weakening operation (20Nm and 4500r/min)

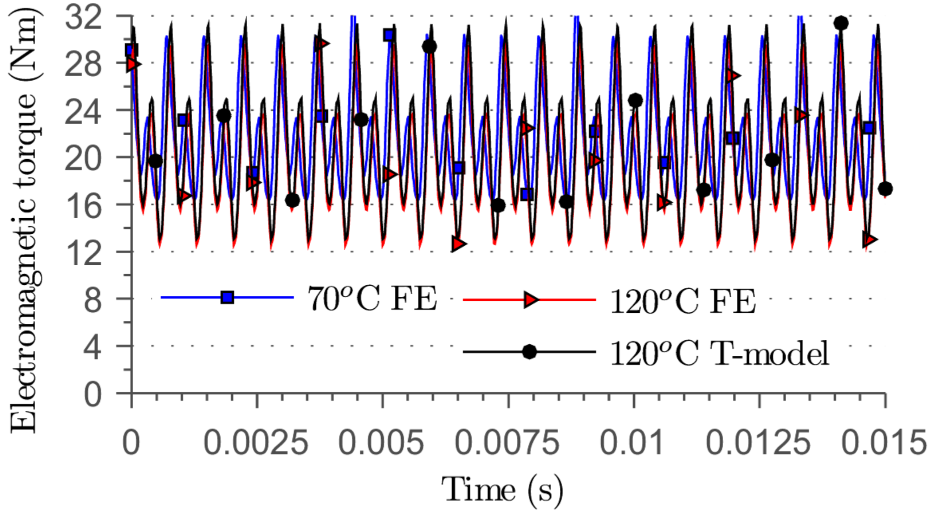

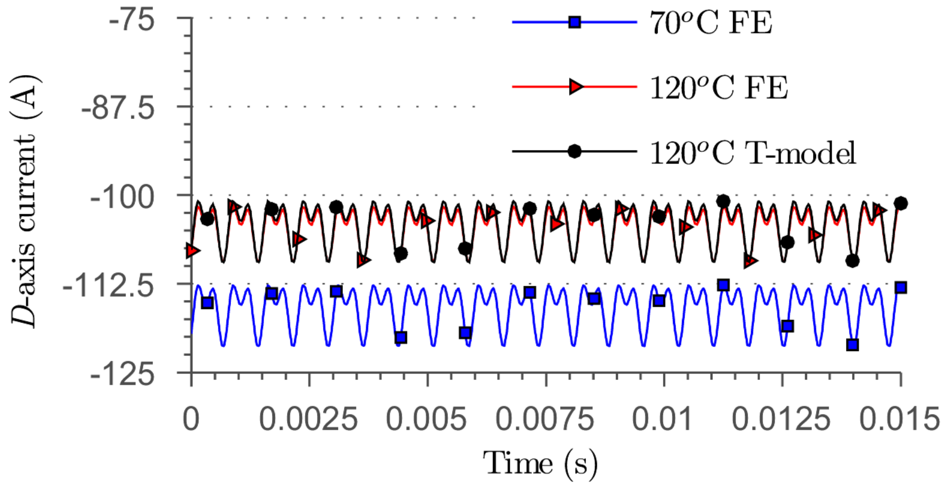

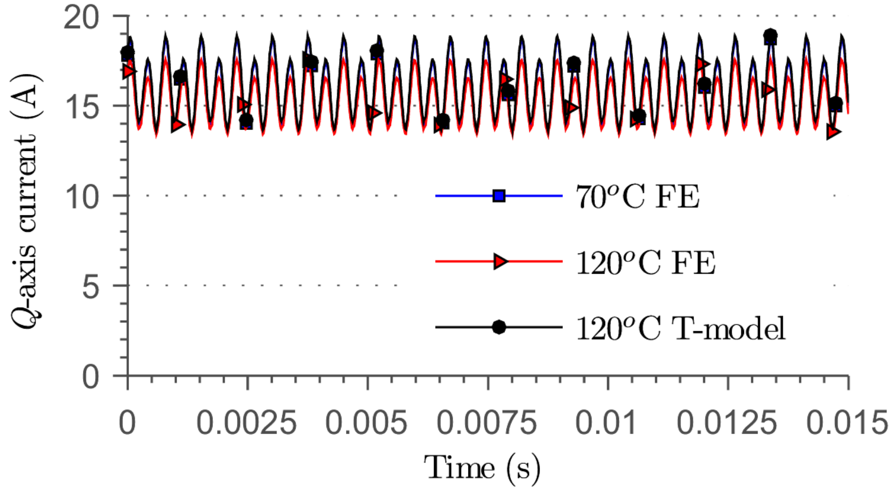

Good agreement achieved

Electro-thermally Coupled Simulation

Winding temperature:

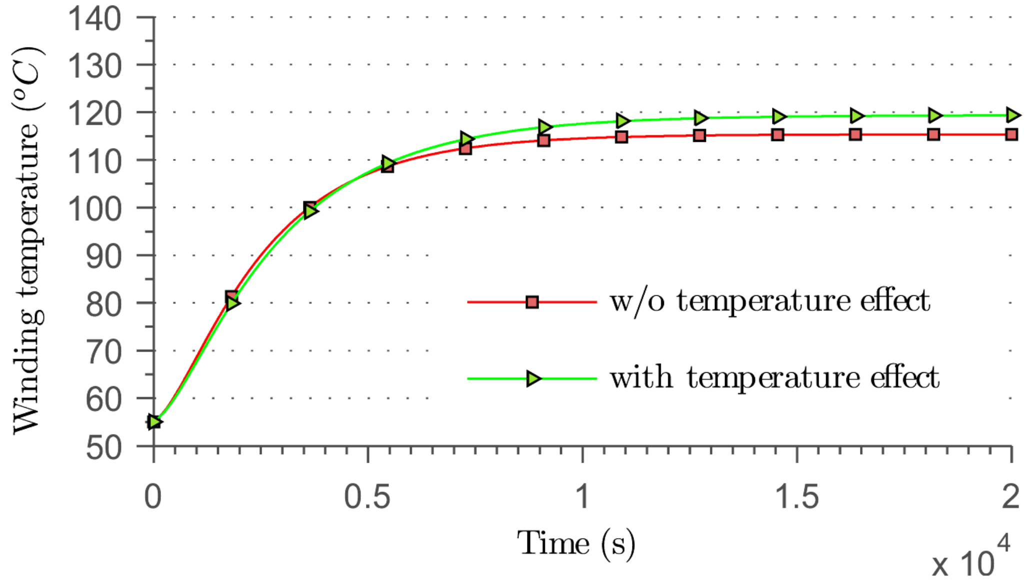

Magnet temperature:

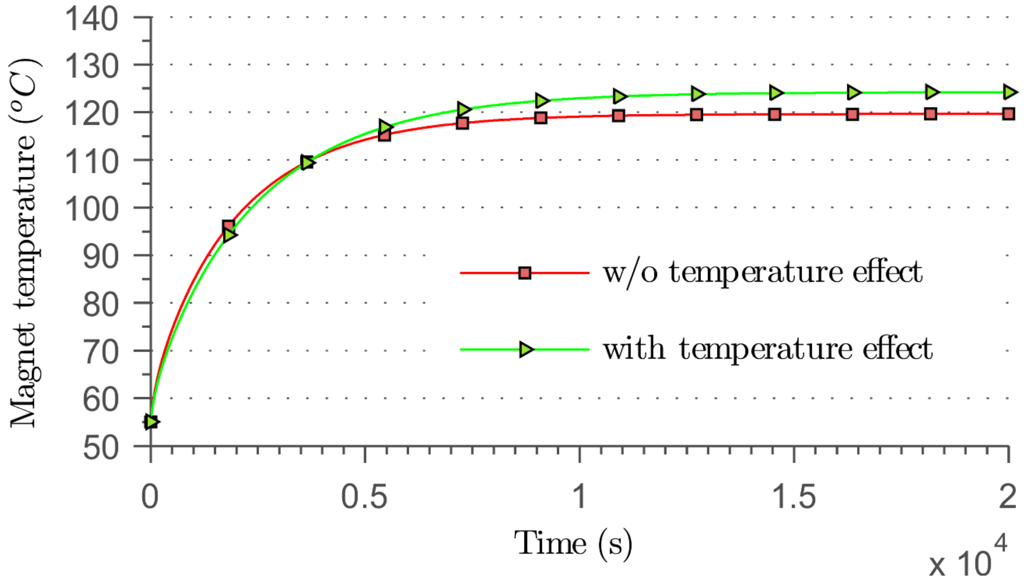

Rated torque and base speed operation
'w/o temperature effect' refers to assuming the machine temperature is fixed at 100°C

With the temperature effect considered, the winding and magnet temperatures are ~5°C higher than the results calculated using the conventional method when the machine gets into thermal steady state.

20 Artemis Urban Driving Cycles, 10° gradient

Winding temperature:

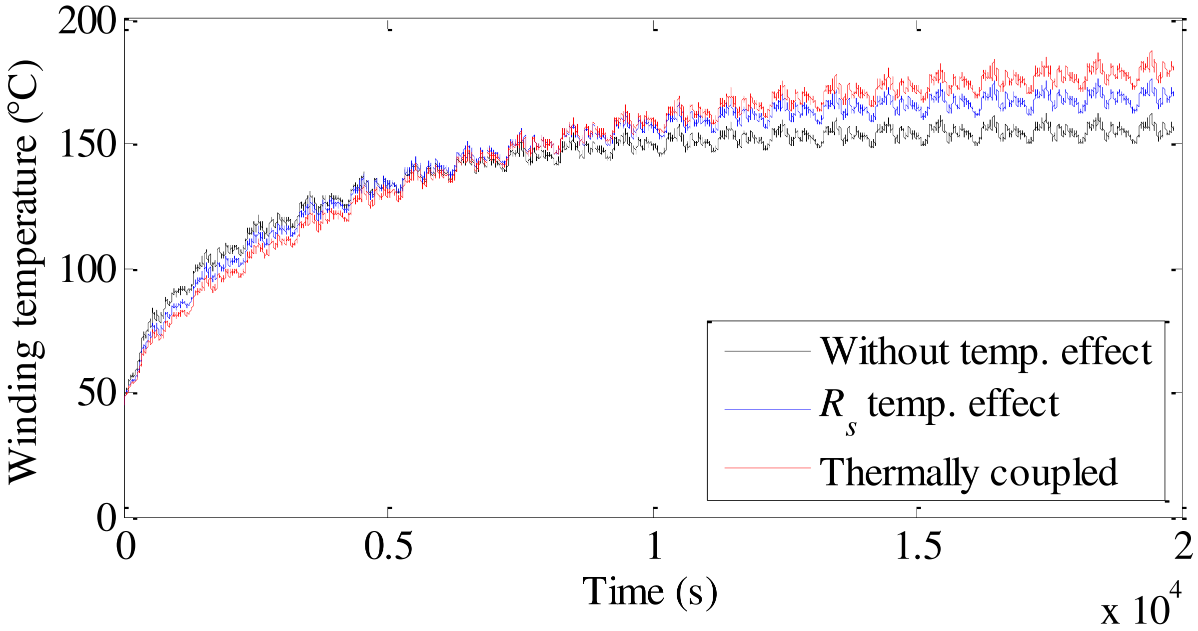

Magnet temperature:

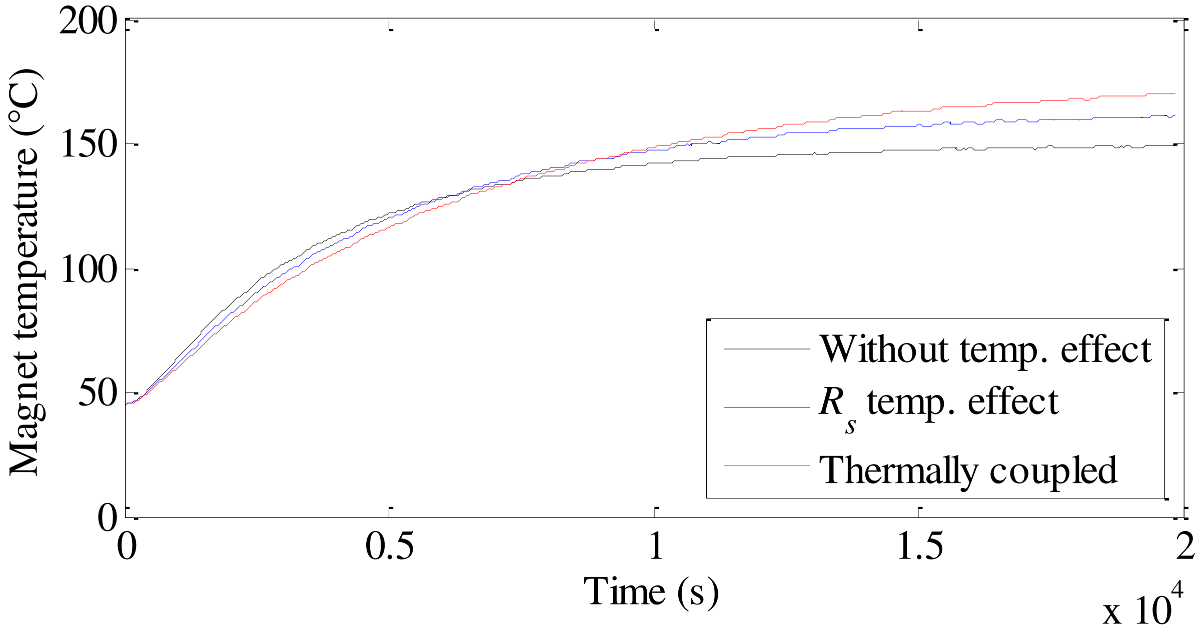

With the temperature effect considered, the winding and magnet temperatures are ~20°C higher than the results calculated using the conventional method and ~10°C higher than the results considering only the temperature effects on winding resistance.

Experimental validation

Test rig

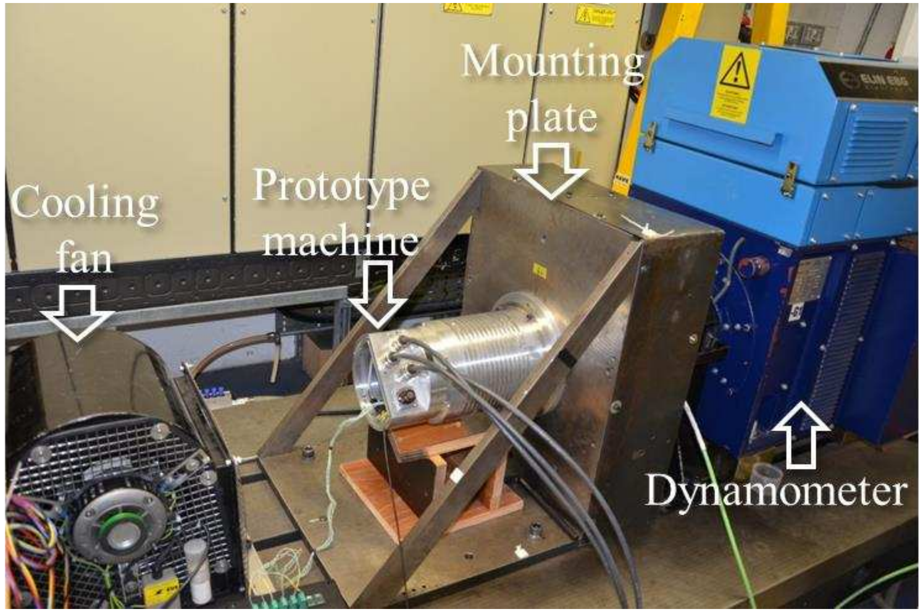

Power resistors:

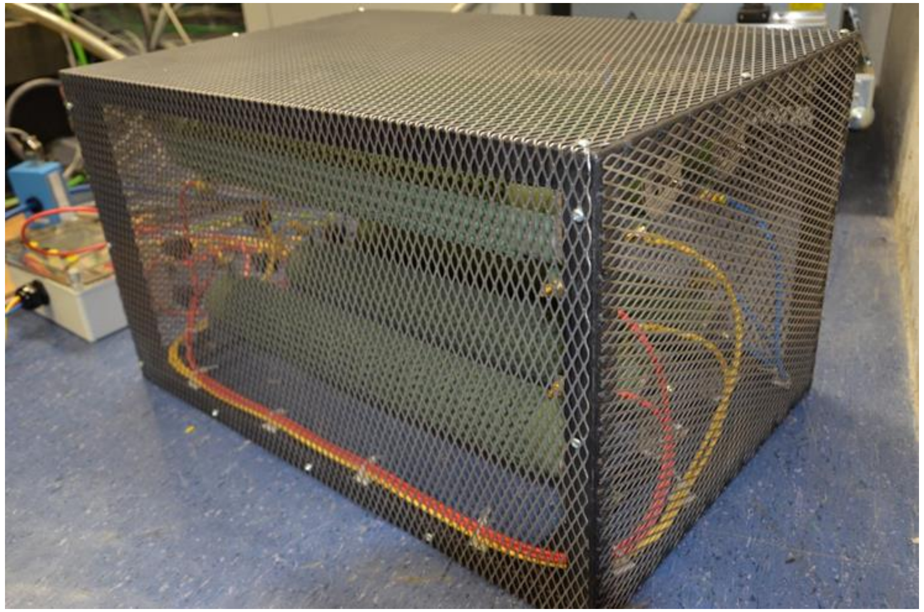

A prototype machine of the 36-slot 6-pole IPM is driven by a dynamometer in the generator mode with a resistive load at different temperatures.

Experimental validation

Back-EMF

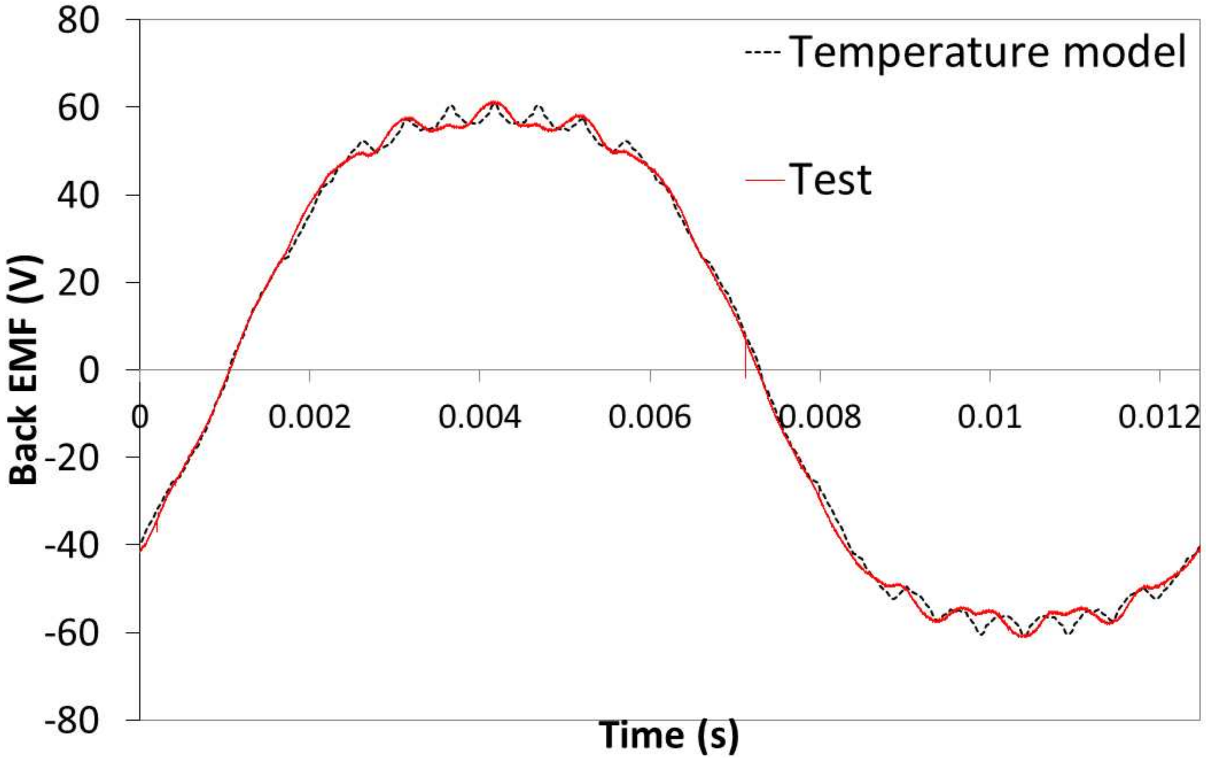

With the calibrated remanence, the predicted open-circuit back EMFs at 20^{o}C have good agreements with the measure ones.

Experimental validation

Current Measurements

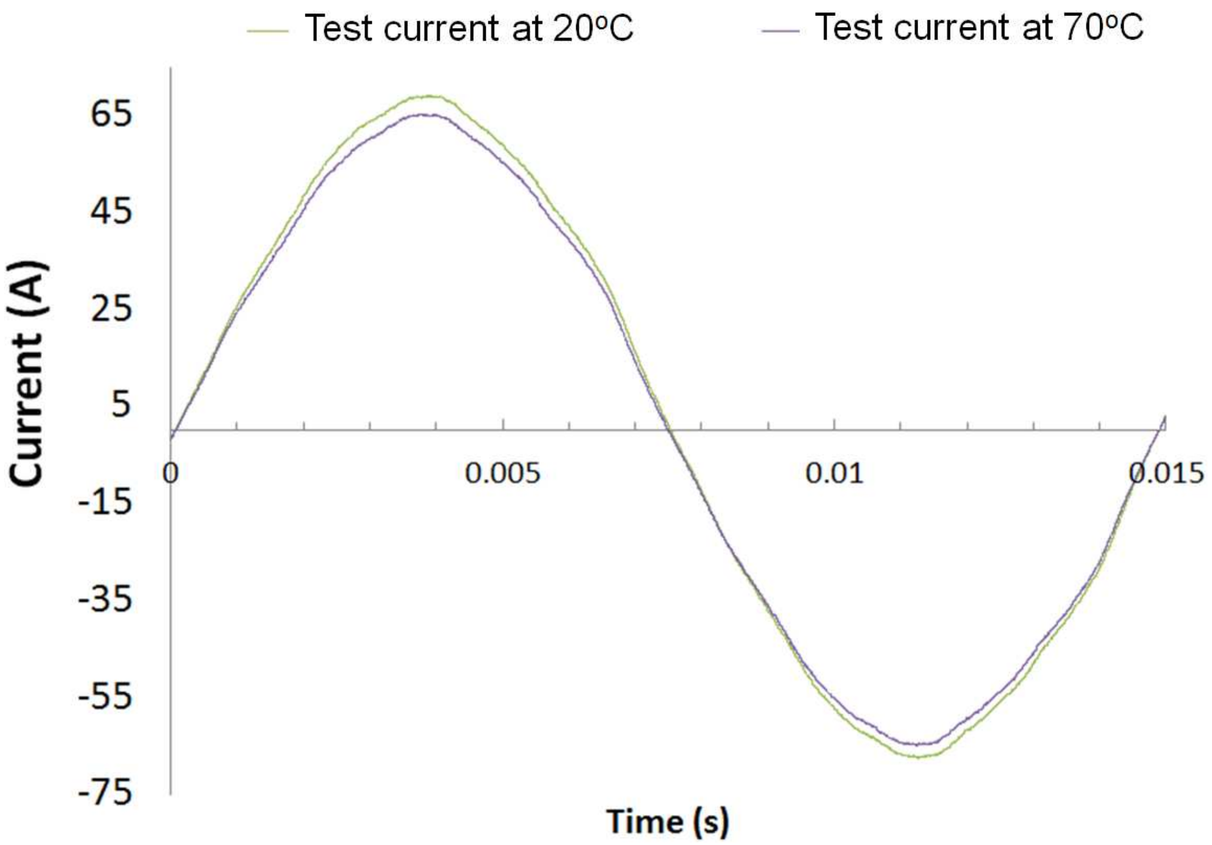

6% reduction in fundamental current when temperature rises from 20^{o}C to 70^{o}C

Experimental validation

Comparison

20°C

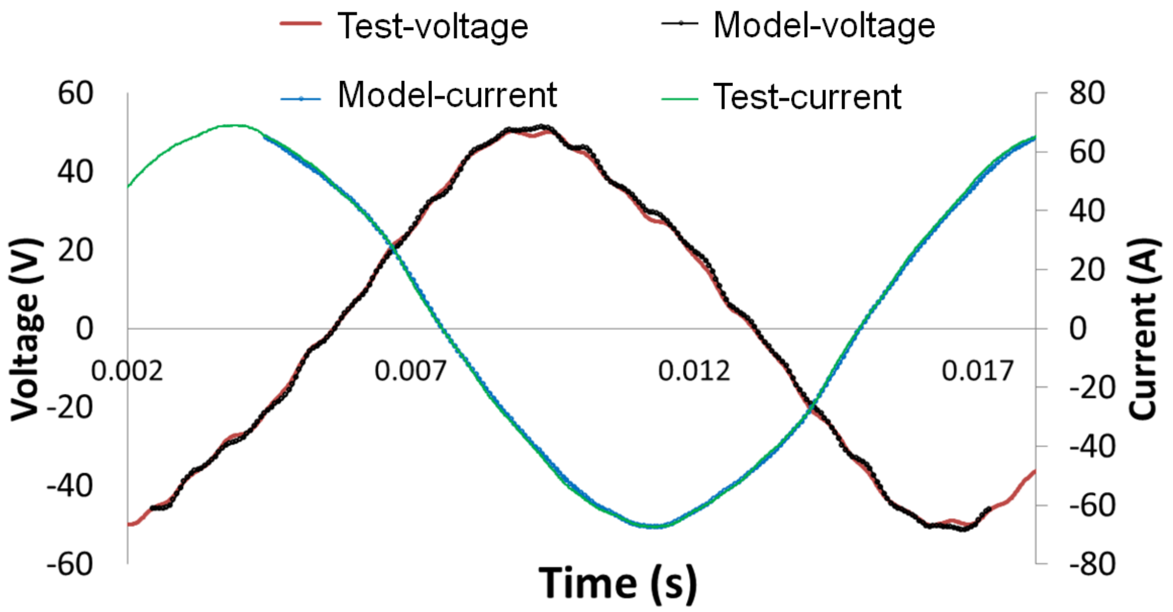

70°C

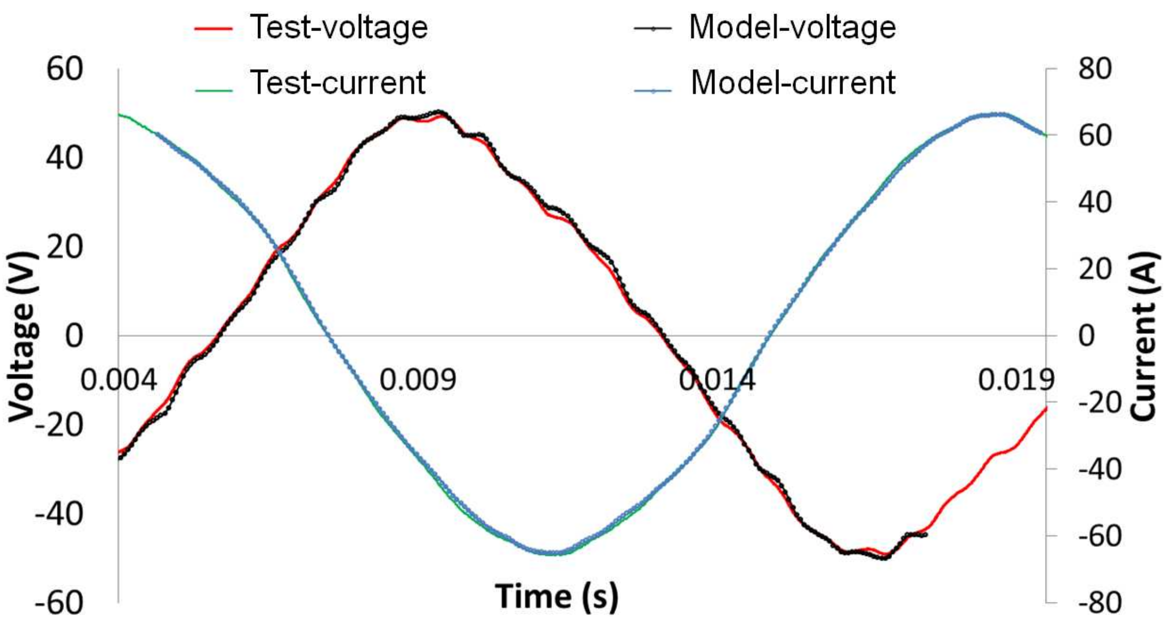

Good agreement achieved

Experimental validation

Measured torque

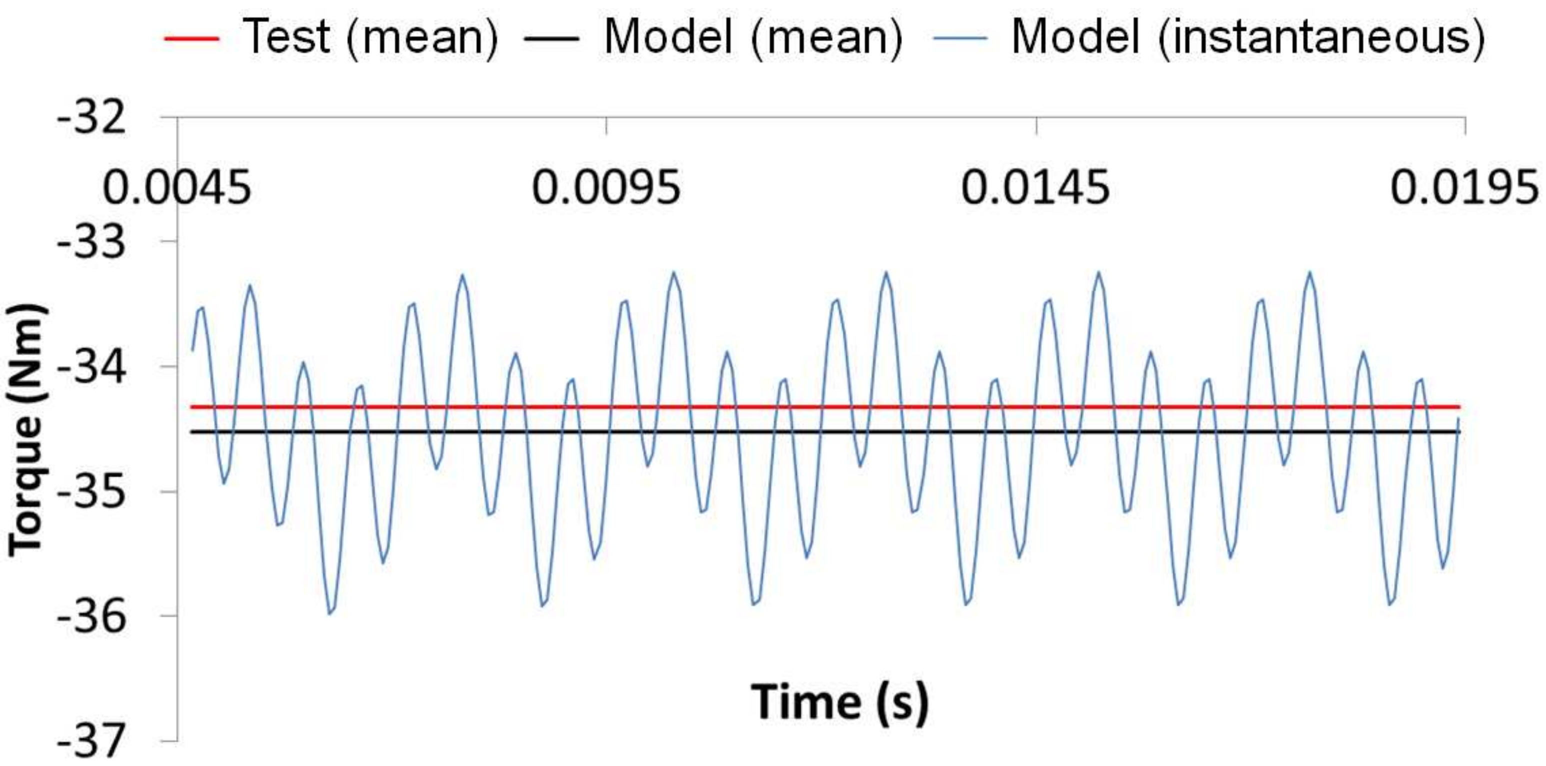

Mean torque error: 0.58%

Conclusions

- This paper proposed a high fidelity, computationally efficient method for representing the temperature effect of magnets on the machine behaviors.
- It employs an equivalent d-axis current proportional to the temperature variations in the machine flux linkage maps characterized at a reference temperature and expressed as functions of d- and q-axis currents and rotor position.
- The method can greatly reduce simulation time for performance evaluation under driving cycles various driving conditions.
- The effectiveness of the method has been validated by finite element analysis and tests on a prototype machine.

Thank you for your attention!